The Exo-S probe class starshade mission

The Exo-S Probe Class Starshade Mission

Sara Seager*[a], Margaret Turnbull[b], William Sparks[c], Mark Thomson[d], Stuart B Shaklan[d], Aki Roberge[e], Marc Kuchner[e], N. Jeremy Kasdin[f], Shawn Domagal-Goldman[e], Webster Cash[g], Keith Warfield[d], Doug Lisman[d], Dan Scharf[d], David Webb[d], Rachel Trabert[d], Stefan Martin[d], Eric Cady[d], Cate Heneghan[d]

[a]Massachusetts Institute of Technology, 77 Massachusetts Avenue, Cambridge, MA, USA 02139-4307; [b]Global Science Institute, P.O. Box 252, Antigo, WI, USA 54409; [c]Space Telescope Science Institute, 3700 San Martin Drive, Baltimore, MD, USA 21218-2410; [d]Jet Propulsion Laboratory, California Institute of Technology, 4800 Oak Grove Drive, Pasadena, CA, USA 91109-8001; [e]Goddard Space Flight Center, 8800 Greenbelt Road, Greenbelt, MD, USA 20771-2400;[f]Princeton University, Department of Mechanical and Aerospace Engineering, Engineering Quadrangle, Olden Street, Princeton, NJ, USA 08544; [g]University of Colorado, Center for Astrophysics and Space Astronomy, 389 UCB, Boulder, CO, USA 80309-0389

ABSTRACT

Exo-S is a direct imaging space-based mission to discover and characterize exoplanets. With its modest size, Exo-S bridges the gap between census missions like Kepler and a future space-based flagship direct imaging exoplanet mission. With the ability to reach down to Earth-size planets in the habitable zones of nearly two dozen nearby stars, Exo-S is a powerful first step in the search for and identification of Earth-like planets. Compelling science can be returned at the same time as the technological and scientific framework is developed for a larger flagship mission. The Exo-S Science and Technology Definition Team studied two viable starshade-telescope missions for exoplanet direct imaging, targeted to the $1B cost guideline. The first Exo-S mission concept is a starshade and telescope system dedicated to each other for the sole purpose of direct imaging for exoplanets (The "Starshade Dedicated Mission"). The starshade and commercial, 1.1-m diameter telescope co-launch, sharing the same low-cost launch vehicle, conserving cost. The Dedicated mission orbits in a heliocentric, Earth leading, Earth-drift away orbit. The telescope has a conventional instrument package that includes the planet camera, a basic spectrometer, and a guide camera. The second Exo-S mission concept is a starshade that launches separately to rendezvous with an existing on-orbit space telescope (the "Starshade Rendezvous Mission"). The existing telescope adopted for the study is the WFIRST-AFTA (Wide-Field Infrared Survey Telescope Astrophysics Focused Telescope Asset). The WFIRST-AFTA 2.4-m telescope is assumed to have previously launched to a Halo orbit about the Earth-Sun L2 point, away from the gravity gradient of Earth orbit which is unsuitable for formation flying of the starshade and telescope. The impact on WFIRST-AFTA for starshade readiness is minimized; the existing coronagraph instrument performs as the starshade science instrument, while formation guidance is handled by the existing coronagraph focal planes with minimal modification and an added transceiver.

Keywords: Exo-S, starshade, external occulter, high contrast imaging, exoplanets

1. INTRODUCTION

Thousands of exoplanets and planet candidates are known to exist and the field of planet discovery continues to funnel towards the discovery and identification of an Earth-like planet. While transits—the pioneering and highly successful Kepler [6] and the upcoming TESS mission [7] —are the exoplanet discovery missions of the current generation, space-based direct imaging is required to ultimately find and identify true Earth analogs: Earth-like planets orbiting Sun-like stars. The starshade mission is a space-based, visible wavelength, direct imaging method to search the nearest Sun-like

*seager@mit.edu; http://seagerexoplanets.mit.edu

Techniques and Instrumentation for Detection of Exoplanets VII, edited by Stuart Shaklan, Proc. of SPIE Vol. 9605
96050W · © 2015 SPIE · CCC code: 0277-786X/15/$18 · doi: 10.1117/12.2190378

stars for planets of all kinds in reflected light, and to characterize both new and already known planets with low-resolution spectra.

1.1 Starshade Conceptual Introduction

A starshade (also called an external occulter) is a spacecraft with a carefully shaped screen flown in formation with a telescope (Figure 1). The starshade size and shape, and the starshade-telescope separation, are designed so that the starshade casts a very dark and highly controlled shadow, suppressing the light from the star while leaving the planet's reflected light unaffected. In this way, only the exoplanet light enters the telescope. Most designs feature a starshade tens of meters in diameter that is separated from the telescope by tens of thousands of kilometers.

One might expect, based only on geometric optics, the starshade to be only a bit larger than the diameter of the telescope aperture, circular in shape, and flying in formation close to the telescope. However, diffraction around a circular occulter results in a degraded shadow that is many orders of magnitude brighter than needed for exoplanet imaging. The degraded shadow could be mitigated by employing a much larger and more distant starshade, but the size and distance rapidly becomes prohibitive. Since the early 1960s, it has been known that a circular screen with a radial apodization at large starshade-telescope separations would create a sufficiently dark shadow with a reasonably sized starshade. While such a radial apodization is not manufacturable with sufficient accuracy, it can be approximated using a ring of petals, leading to the special shape of the starshade. Within the family of solutions for the starshade-telescope separation, and the starshade overall size, petal number and shape, the actual solution chosen and its implementation is ultimately driven by engineering design constraints.

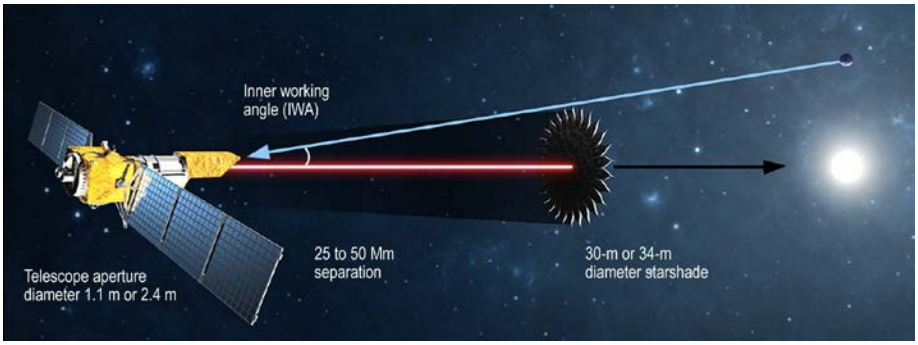

Figure 1. Schematic of the starshade-telescope system (not to scale). Starshade viewing geometry with IWA independent of telescope size.

Starshade strengths. There are several strengths that a starshade approach brings to exoplanet imaging and characterization. Most significantly, the inner working angle (IWA) and the contrast achieved in the telescope image (the reduction in starlight at the planet location) are mainly a function of the starshade size and distance, not the telescope aperture.

A starshade operates by suppressing the light from a parent star before it enters the telescope where it can scatter and hide the very faint planet. Suppression is defined as that fraction of the parent star's light that is allowed to enter the telescope. Contrast is the amount of background signal in a single telescope resolution element expressed as a fraction of the central star's brightness. Contrast can be degraded by scattered and diffracted unsuppressed starlight, exozodiacal light, local zodiacal light, and detector dark noise.

With a starshade, the starlight is almost entirely suppressed, and the IWA limit at which a planet is visible off the limb of the starshade depends only on the size and distance of the starshade. In principle, even a tiny telescope would be adequate for direct imaging of small exoplanets. In practice, the telescope aperture must be sufficiently large to provide adequate signal and low enough noise from the residual limitations on contrast.

Because the starlight never enters the telescope, there is no need for specialized optics to achieve high contrast (which typically reduce throughput), and a relatively simple space telescope is all that is needed. On-axis obstructions or mirror

segments do not interfere with starlight cancellation and wavefront correction is not required (which frees the telescope from tight thermo-mechanical requirements).

An additional significant feature of the starshade-telescope system is the absence of an outer working angle (OWA). A 360° suppressed field of view (FOV) with angles from the star limited only by the detector size is obtained with each image. This is particularly useful for imaging debris disks or planets at large orbital separations, thereby studying planetary systems as a whole.

The starshade works over a broad bandpass. Numerically optimized designs balance the desired bandpass with other science drivers and engineering constraints. Hypergaussian designs have no lower limit to their bandpass.

The starshade-telescope system can detect Earth-size planets in the habitable zone of Sun-like stars (see Figure 2) even with a small telescope (on order of 1- to 2-m aperture diameter). This ambitious statement is allowed by the fact that nearly all of the starlight suppression is done by the starshade. As long as the tolerances for starshade petal precision manufacturing, deployment, and formation flying control are met, the Exo-S mission will be capable of reaching the 10^{-10} contrast level needed to directly observe Earth analog exoplanets around Sun-like stars. An important related point supporting starshades with small telescopes is that wavefront correction is not required. If high-precision wavefront correction were required, the telescope collecting area would be a limiting factor on the starlight suppression, since wavefront sensing and control relies on collecting enough target starlight to sense the time-dependent optical imperfections that need to be corrected. In the wavefront correction case, small telescopes put Earth-Sun flux contrast levels out of reach.

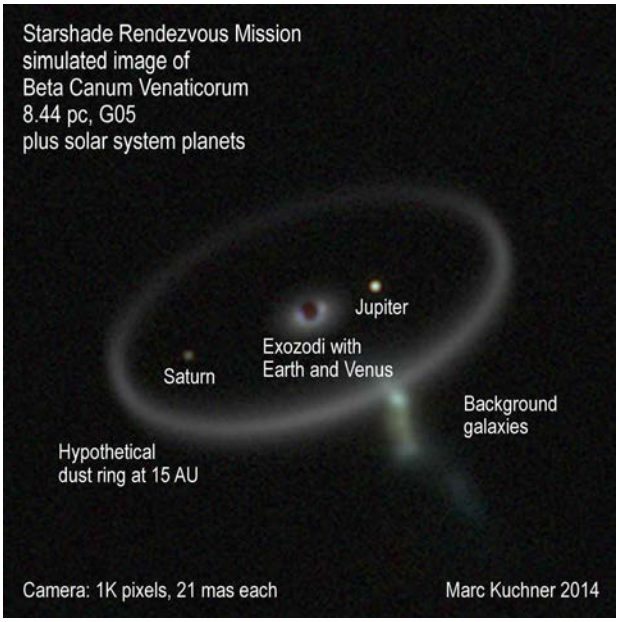

Figure 2. Simulated image of the Rendezvous Mission's observation of a solar-system–like planetary system orbiting a nearby Sun-like star. The image is a composite of three bands (510, 658, 825 nm), square-root scaled and mapped to blue, green, and red to create a false-color image. The planets in this simulation are all placed at quadrature, with albedos (and colors) taken from [1] and adopting a Lambertian scattering phase function. The simulation includes photon noise, read noise of 2.8 e-/pixel and dark current of 5.5e-4 e-/pix/sec, assumes a total throughput of 20% and a 2000 second read cadence. For reference, with these assumptions, the Venus twin in this system is detected at a signal to noise ratio of about 12. The model for background galaxies was generated with the Illustris cosmological simulation [5] converted to mock images using stellar population synthesis models [8]. (Courtesy of Gregory Snyder at the Space Telescope Science Institute).

The starshade's powerful capability for starlight suppression means the challenges of reaching the required IWA all lie with the starshade. The contrast, on the other hand, is limited by the convolution of the telescope response with the unsuppressed light, the internal telescope noise, and the sources of background from the sky. The challenges associated with producing a successful telescope-starshade system can be divided into "programmatic challenges" (below) and "technical challenges" (Section 6).

Starshade challenges. The starshade represents a new kind of system, one that has never been flow before, and therefore presents unique programmatic challenges. First, a full-scale, ground-based end-to-end system test for the starshade-telescope system is impossible because of the large size of the occulting screen (tens of meters), the large separation distances between the telescope and starshade (tens of thousands of kilometers), and the guidance, navigation, and control (GN&C) formation flying requirements. Subscale testing (see Section 6.2), together with computer performance modeling and simulations is the only alternative.

The second programmatic challenge is operational: for a given mission duration, the starshade has a limited number of retarget maneuvers (on the order of 30 per year) due to retarget times (from several days to a couple of weeks) and fuel constraints, meaning that only a limited number of stars can be observed over the mission duration. More than one

starshade can lessen, but not remove, the problem of limited number of target stars. For a shared telescope, the retargeting time would be used for general astrophysics observations, allowing about 25% of telescope time for exoplanet direct imaging.

1.2 Starshade History

The idea of using an (apodized) starshade to image planets was first proposed in 1962 by Lyman Spitzer at Princeton [9]. In this landmark paper (in which he also suggested that NASA build and fly what would later became the Hubble Space Telescope and the Chandra Observatory), he proposed that an external occulting disk could be used to block most of the starlight from reaching the telescope, thus enabling the direct imaging of planets around nearby stars. He realized that diffraction from a circular disk would be problematic for imaging an Earth-like planet due to an insufficient level of light suppression across the telescope's pupil. He posited that a different edge shape could be used instead, foreshadowing today's approach. In 1974, the idea was revived by G.R. Woodcock of the Goddard Space Flight Center using apodized starshades. In 1985, Marchal [10] discussed the use of an opaque disk surrounded shaped petals, but while they were impractically large, they foreshadowed the modern design.

In 1995, the floodgates of exoplanet discovery were opened and interest in occulters grew. Several mission concepts were proposed using apodized starshades. Copi and Starkman in 2000 [11] revisited the apodized starshade and found transmissive solutions defined by polynomials; their proposed mission was called the Big Occulting Steerable Satellite (BOSS). A few years later, Schultz et al. [12] proposed a similar mission dubbed UMBRAS (Umbral Missions Blocking Radiating Astronomical Sources). However, these suggestions were hampered by the difficulty in manufacturing a transmissive surface within the tight tolerances necessary. In 2004, Simmons [13, 14] again looked at using starshades based on shaped pupil designs and suggested that the star-shaped design [15] was promising.

Then, in 2006, Cash [16] showed that an occulter consisting of an opaque solid inner disk surrounded by petals forming an offset hypergaussian function, tip-to-tip about 60 m in diameter, created a broadband, deep shadow. With a small IWA and reasonable manufacturing tolerances, this design finally allowed for the possibility of an affordable solution.

Designs based on a solid inner disk and shaped petals form the basis of several variations in the apodization function. In 2007 Vancderbei et al. [17] developed a non-parametric, numerically generated approach to petal shape design. The resulting numerical designs allow for optimization considering engineering constraints such as petal tip and valley width, petal length, and overall diameter, while preserving desired science performance.

In 2008, two teams were selected under the Astrophysics Strategic Mission Concept Study (ASMCS) to study starshades. Cash et al. [18] reported on the New Worlds Observer, while Kasdin et al. [19] described THEIA. Both missions were proposed with a 4-m- diameter telescope coupled with a starshade to achieve the sensitivity required to characterize Earth-like planets in the habitable zones of their parent stars.

1.3 Exo-S Probe-Class Study

The Exo-Starshade (Exo-S) Science and Technology Definition Team (STDT) is tasked by NASA to study the starshade-telescope mission concept under the "Probe" class of space missions, with a targeted cost of $1B (FY15 dollars). Per the STDT charter, the mission should be ready for a "new start" in 2017, with launch in 2024, and science beyond the expected ground capability at the end of the mission. The Exo-S mission concept study began in May 2013 and ran until delivery of the Final Report in March 2015. Two mission concepts were studied. The "Starshade Dedicated Mission" is a starshade and commercial, 1.1-m diameter telescope that are co-launched, sharing the same low-cost launch vehicle, conserving cost. The Dedicated mission orbits in a heliocentric, Earth leading, Earth-drift away orbit. The telescope has a conventional instrument package that includes the planet camera, a basic spectrometer, and a guide camera. The "Starshade Rendezvous Mission" is a starshade that launches separately to rendezvous with an existing on orbit space telescope. The existing telescope adopted for the Exo-S study is the WFIRST-AFTA (Wide-Field Infrared Survey Telescope Astrophysics Focused Telescope Asset). The WFIRST-AFTA 2.4-m telescope is assumed to have previously launched to a Halo orbit about the Earth-Sun L2 point. While the Dedicated Mission was the original goal for the Exo-S study, the Rendezvous mission is far more compelling because the larger telescope aperture has more capability for planet discovery and characterization. The Exo-S Final Report can be found at http://exep.jpl.nasa.gov/stdt/Exo-S_Starshade_Probe_Class_Final_Report_150312_URS250118.pdf (and for the concurrent Exo-C Final Report see http://exep.jpl.nasa.gov/stdt/Exo-C_Final_Report_for_Unlimited_Release_150323.pdf).

2. SCIENCE GOALS AND OBSERVING PROGRAM

2.1 Science Goals

The Exo-S mission has four science goals. The first goal is *to discover new planets from Earth size to giant planets.* Within this goal is the possibility of discovering Earth-size exoplanets in the habitable zones (HZ) of at least 10 Sun-like stars—arguably one of the most exciting pursuits in exoplanet research.

The second science goal is *to measure spectra of a subset of newly discovered planets.* The Exo-S spectral range is from 400–1,000 nm, with a spectral resolution of up to R=70, which enables detection of key spectral features. Of particular interest are the so-called sub-Neptunes, planets with no solar system counterparts, loosely defined as 1.75 to 3 times the size of Earth. The sub-Neptune planets have very low densities compared to Earth, yet their actual composition is not known. (See Figure 3.)

The third science goal is designed to guarantee outstanding science return: *to characterize known giant planets, by observing their spectra and measuring or constraining planet mass.* The known giant planets are detectable by virtue of extrapolated position in the 2024 timeframe. Molecular composition and the presence/absence of clouds or hazes will yield information on the diversity of giant planet atmospheres.

The fourth science goal is *to characterize planetary systems, with a specific interest in studying circumstellar dust in the context of known planets*. Observations will shed light on the dust-generating parent bodies (asteroids and comets), and the dynamical history of the system, as well as possibly point to unseen planets below the mission's direct detection thresholds. An assessment of dust levels in the habitable zones of nearby stars is a major unknown affecting mission planning for future flagship mission concepts.

To illustrate what data from the Exo-S will look like, a simulated image for the Rendezvous Mission is presented in Figure 2. The image shows a hypothetical planetary system around the nearby (8.44 pc) G0 V star Beta Canum Venaticorum if it contained all eight solar system planets, a cloud of warm dust comparable to the solar zodiacal cloud (1 zodi) and a dust ring from a Kuiper belt located 15 AU from the star. The center of the image is blocked by the starshade.

The brightness of the giant planet Jupiter analog (just to the right of image center) vivifies Exo-S's science goal of characterizing known giant planets; this planet creates the brightest pixel in the image by far. The Saturn analog (the bright point left of image center) and the terrestrial planet analogs Earth and Venus illustrate the Exo-S mission's capability to discover new planets. The Earth and Venus analogs appear as colored peaks (left and right respectively) on top of the exozodiacal dust.

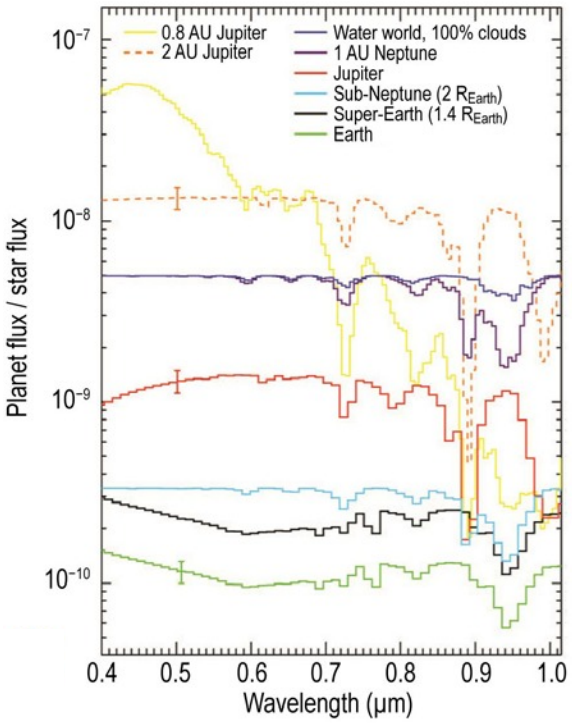

Figure 3. Exoplanet spectra showing the differences and similarities in brightness and spectral features for a variety of exoplanet types. Optical reflectance spectra of a diverse suite of exoplanets are shown without added noise. The Jupiter spectrum is based on the observed spectrum in [2]. The other two Jovian planet spectra are models from [3]. The Neptunian and water world spectra are models from Renyu Hu (personal communication). The Earth spectrum is a model developed to match Earth observations from the EPOXI mission [4], while the super Earth is that model scaled by $(1.5\ R_{Earth}/1\ R_{Earth})^2$. This Figure is for the 2.4-m Rendezvous Mission, and the plots roughly represent the best spectra possible. There are 2 pixels per resolution element (Nyquist sampling). For the Rendezvous Mission plot, all spectra were convolved to a spectral resolution of 70. Three representative flux error bars are placed at 0.5 μm. The errors are the noise per pixel for spectra with SNR=10 per resolution element. Image credit: A. Roberge.

The exozodiacal dust cloud is the bright ring at the image center. Exozodiacal dust is a challenge for all planet-imaging missions. Although the peak of the exozodiacal signal in this scene is comparable to the brightness of the Venus spot, the image of Earth is about twice as bright as the exozodiacal light background in that pixel. Vivid images of a complete dust

ring made by the starshade will help constrain the scattering phase function of the dust, which in turn should enable some level of subtraction of the dust signal from the planet light.

Exo-S will observe different components of planetary systems as illustrated by the hypothetical Kuiper belt dust ring at 15 AU from the star. Exo-S will likely discover and make spectacular images of such cold dust rings around some of the target stars. The dust ring in the image is brighter than the Kuiper belt but fainter than prior survey limits [20].

Direct imaging exoplanet science is a daunting task not afforded justice by a few outlined goals. Several pressing astrophysical questions have come to the forefront, including: how much can be learned about planets with limited spectral and temporal information; how planets can be efficiently distinguished from background sources; how stray light from binary stars should be handled; and how exozodiacal dust levels higher than the solar system's might impact the science harvest of a direct imaging mission. Answering these concerns requires a large-scale dedicated effort in the coming years.

2.2 Sample Observing Program and Planet Yields

The science goals are carried out by an observing program, created from balancing the search for new exoplanets with the spectral characterization of known giant exoplanets. A key factor is the time and fuel it takes to align the starshade and telescope system to observe the next target star, and therefore the number of possible retargets available within the mission lifetime. The science yield, in terms of how many planets are discovered and to what spectral resolution small planet atmospheres can be characterized depends both on the observing strategy (how the finite number of starshade retargets are allocated) and the telescope aperture.

A Design Reference Mission (DRM) describes the sequence of observations to be performed and estimates the numbers of planets that will be detected and characterized. It is executed with a Matlab-based tool developed for the Exo-S study.

The Exo-S DRM employs a hierarchical approach: an observation schedule of known giant planets, whose availabilities for observation are known from their orbital parameters, forms a "framework" of observations that have a high probability of success. In between observations of known giant planet, the next set of highest priority stars are scheduled. These stars are selected in one of two programs that focus on either Earth twins in the habitable zone of Sun-like stars (here Earth twin is defined as an Earth-sized planet with Earth's

Planet Type	Completeness
HZ Earth	10.9
Earth	3.7
Super Earth	27.3
Sub-Neptune	52.3
Neptune	71.1
Jupiter	93.9
Total	259.2
	Yield
HZ Earth	1.7
Earth	0.6
Super Earth	2.7
Sub-Neptune	5.2
Neptune	7.1
Jupiter	9.4
Known Jupiters	12
Total	38.8

Table 1. Planet completeness and yield for the Rendezvous Mission with emphasis on exoEarths.

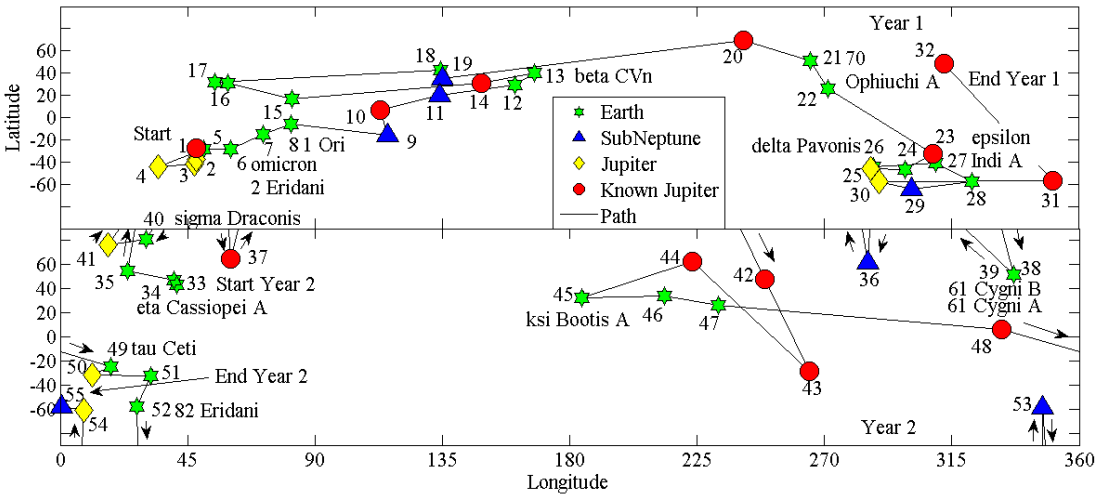

Figure 4. Observing sequence for the Rendezvous Mission with an emphasis on Earth twins in the habitable zone. Coordinates are ecliptic longitude and latitude

geometric albedo of 0.2) or a set of high-priority, high-completeness stars. Observations of lower priority targets are assigned in this way until all the time is accounted for in single-visit scenarios of two years. The Exo-S DRM [21] differs from several precedent starshade DRMs that focus on detection and/or characterization of Earth twins for various mission optimizations [22-25].

An input star list is used to design an efficient observing sequence. Each target star is observed once during the first two years of the mission. The list and number of target stars (ranging from 40 to 55 for the two years) and the predicted planet yield, depends on the strategy for types of planets to be harvested and telescope aperture. Three different case studies are presented in this report. The third year of the Exo-S mission is reserved for follow-on observations, for confirmation of potential detections and spectroscopic observations. The actual observing schedule is adaptable to real-time discoveries. A sample observing sequence is shown in Figure 4. The planet completeness and yield and completeness are shown in Table 1, and are based on the following parameters: luminosity-based limiting magnitude [a limiting contrast ratio expressed in magnitudes is $\lim\Delta mag = 25.5 + 2.5\log L$, for $L<1.6$, and $\lim\Delta mag = 26$ (a contrast ratio of 4×10^{-11}, the instrument's sensitivity limit) for higher luminosity stars]; IWA=71 mas blue band for 12 habitable Earth-twin candidates and the IWA=100 green band for the other candidates; local zodi of 23 mag/sq. arcseconds; exozodi of 6 times local zodi; planet sizes in Earth radii/geometric albedos as follows (Earths 1/0.2; super Earths (1.4/0.2); sub Neptunes 2/various; Neptunes 3.9/various; Jupiters 11/various). For more details about the Exo-S DRM see [21].

3. STARSHADE DESIGN

3.1 Starshade Sizing and Optical Design

The starshade's purpose is to create a deep shadow at the aperture of a space telescope by blocking starlight and limiting starlight diffracting into the shadow region. There is an infinite family of flower-like starshade shapes that produce a dark shadow suitable for planet hunting given a large enough starshade. To find these shapes, designers began by writing down analytic functions with a few parameters (e.g., [11, 16]). Later, [17] introduced more complex shapes with hundreds of parameters defining the edge shapes, and used linear optimization to choose the parameter values. Further design requirements beyond starlight suppression are set by other scientific and engineering considerations (e.g., disk diameter and petal length limitations, minimum feature sizes, bandpasses) constraining the many degrees of freedom in this optimization.

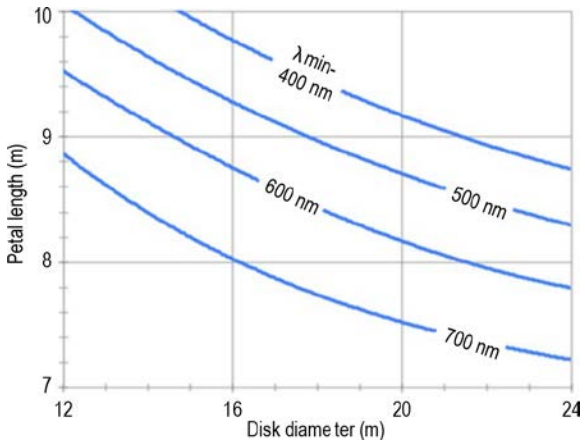

Figure 5. Starshade dimensions vs. bandpass lower limits. The starshade has: an upper bandpass limit of 1,000 nm, 100 mas IWA, $\lim\Delta mag$ =26, 3.1-m shadow. Large starshades are required to cover the full (400–1000 nm) bandpass.

For the Exo-S study, a three-step optical design process was employed in iterative fashion to find an optimal solution. First, parametric studies were conducted based on a large number of approximate solutions and curve fitting to illustrate trends. Second, some tens of potential designs were run through the optimization scheme to identify candidates with high suppression and consistency with all imposed constraints. Finally, select designs were rigorously verified to provide the requisite starlight suppression at all points in the focal plane. Parameters were adjusted until the design is fully compliant with requirements imposed by scientific constraints (IWA=100 mas, planet-star flux contrast, and spectral band pass 400 - 1000 nm) and engineering constraints (truss diameter and mechanical factors such as a physical limit on the petal length/width aspect ratio, a requirement on petal stiffness, and a limit on the overall length of the starshade petal).

There is freedom in the starshade size vs. band pass range. For a starshade design that meets the requirements of an IWA of 100 mas, and a minimum planet sensitivity at $\lim\Delta mag = 26$, there are two choices to address the required spectral coverage: design a large ~40-m starshade (e.g., 20-m central disk with 9.2-m-long petals) capable of covering the full 400–1,000 nm range (Figure 5) from a single separation distance, or design a more compact starshade that covers a portion of the range, and then change the spacecraft separation distance to move this partial bandpass over the full,

required spectral range. While generally offering better performance, larger starshades weigh more, cost more, are slower to reposition, require more fuel to reposition, and—for those much greater than about 35-m minimum diameter—have a weaker heritage case when compared to flight-proven deployable antennas. Large starshades add to mass and packaging issues. Additionally, large designs depart from the to-date technology work. Finally, an early Cost and Technical Evaluation (CATE) risk assessment strongly recommended that the starshade size be kept as small as possible to maintain heritage with low-cost deployable communications antennas. Larger starshade designs were viewed as having greater cost risk. With all these issues considered, the architecture trades were constrained to smaller, partial bandpass starshade designs.

There is a small amount of freedom in selecting the number of petals used. The total number of petals is only bounded weakly by optical considerations—too few petals and terms ignored in the binary apodization approximation slowly begin to become important. Conversely, an increased number of petals makes for smaller petal tips and smaller gaps between petals, as well as simply more hardware to manufacture, test, and deploy. Additional constraints include a minimum petal tip width and inter-petal gap of 1 mm, maximum petal lengths and widths that can be packaged for launch, and upper and lower bounds on the bandpass of operation.

Ultimately, specific point designs are further evaluated for science performance based on the combination of parameters. Planet yield is evaluated for a target list constrained by a candidate starshade's estimated IWA and contrast. Heritage limited the inner disk diameter to 15 m for the Dedicated Mission and to 20 m for the Rendezvous Mission. The Dedicated Mission starshade is designed to produce a 3.1-m-diameter shadow (±1 m around a 1.1-m aperture) for planet sensitivity at 26 magnitudes, IWA of 102 mas, and a primary bandpass of 510–825 nm. This "green band" is chosen as the baseline because it covers prominent spectral features while maintaining an acceptable IWA and a mid-range separation. The starshade can be moved toward or away from the telescope to change the useful bandpass and IWA. Three distance/wavelength pairs are shown in Table 2. Each band provides identical suppression at the telescope aperture at the designated separation distance and IWA; separation distance increases in inverse proportion to wavelength to preserve the same optical performance. The "blue band" is useful to explore closer to the star and increase the number of candidate targets for the Earth-twin survey. The "red band" from 618–1000 nm has access to additional important spectral features, although it carries a corresponding increase of IWA to 118 mas. The Rendezvous Mission starshade is designed to produce a 4.4-m-diameter shadow (±1 m around a 2.4-m aperture) for planet sensitivity at 26 magnitudes and IWA of 100 mas Petal optical length is 7 m, with an inner disk diameter of 20 m and with 28 petals. The Rendezvous Mission design bands are listed in Table 2, and differ from the Dedicated Mission in order minimize the impact to the WFIRST-AFTA existing coronagraph instrument properties.

Case Study	Parameters	Observing Bands		
		Blue	Green	Red
Rendezvous Mission	Bandpass (nm)	425–602	600–850	706–1000
20-m inner disk	IWA (mas)	71	100	118
28 7-m petals	Separation (Mm)	50	35	30
Dedicated Mission	Bandpass (nm)	400–647	510–825	618–1000
16-m inner disk	IWA (mas)	80	102	124
22 7-m petals	Separation (Mm)	39	30	25

Table 2. Summary of starshade and bandpass parameters.

3.2 Starshade Mechanical Design and Heritage

From a mechanical point of view, the starshade is a deployable structure that, upon expansion, creates the requisite optical shape needed to cast a deep shadow on the observing telescope. The starshade is composed of three main elements: the circular inner disk structure (IDS), the petals mounted to the circumference of the IDS, and the opaque optical shield (OS) which covers nearly all of the structure. An example starshade is shown in Figure 6.

The starshade's mechanical architecture is constrained in a number of ways. The structure must fit within a 5-m fairing (along with its enabling spacecraft and a second, telescope-carrying spacecraft) then deploy into a 30-m optical mask once on orbit. It must meet the tight manufacturing and environmental performance tolerances identified in the overall system error budget. Finally, the architecture must meet challenging cost and schedule programmatic constraints. All of these requirements have limited the starshade architectural tradespace and have shaped the starshade designs used in the Exo-S study.

Only a limited number of large deployable structure architectures were considered as part of the Exo-S study due to the cost-driven, time-driven need for heritage from a prior space application; a completely new structural architecture would not meet the Probe Study charter requirement of reaching TRL 5 by 2017. Possible architectures were largely drawn

from industrial experience with large deployable antenna structures. Additionally, the deployable boom architecture (used on the James Webb Space Telescope's thermal shield) was also considered but was dropped due to fairing packaging difficulties in the Dedicated Mission's co-launched configuration. This architecture may be workable for a differently constrained situation and is currently in use for starshade concepts under development by Northrup Grumman.

Historically, deployable mechanical antenna structures come in two designs: radial rib and perimeter truss. Elements of both can be found in the starshade design. The inner disk structure is fundamentally a perimeter truss structure used successfully in deployable space antennas of approximately the same size. Battens have been reduced in length since space to hold the parabolic antenna surface is no longer a design consideration, and spokes have been added to help provide the required deployed stiffness. The end result is a deployed configuration similar in appearance to a bicycle wheel. The petal stowing method draws from flight-proven radial wrapped-rib antennas that stow about a central cylinder. The result is a compactly stowed design in which the starshade IDS and petals stow concentrically around a central, load-bearing cylinder (hub) as seen in Figure 7.

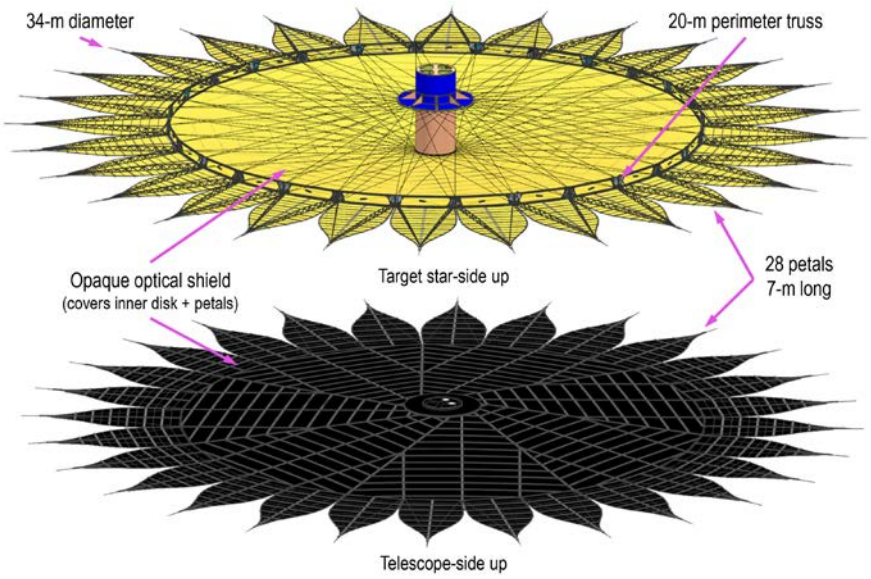

Figure 6. Fully deployed Rendezvous Mission starshade configuration and major system elements.

A further consideration in the starshade architecture is the length-to-width aspect ratio of the petals. Lower ratios make for stiffer petals and better enable the starshade to meet the mechanical performance requirements identified in the error

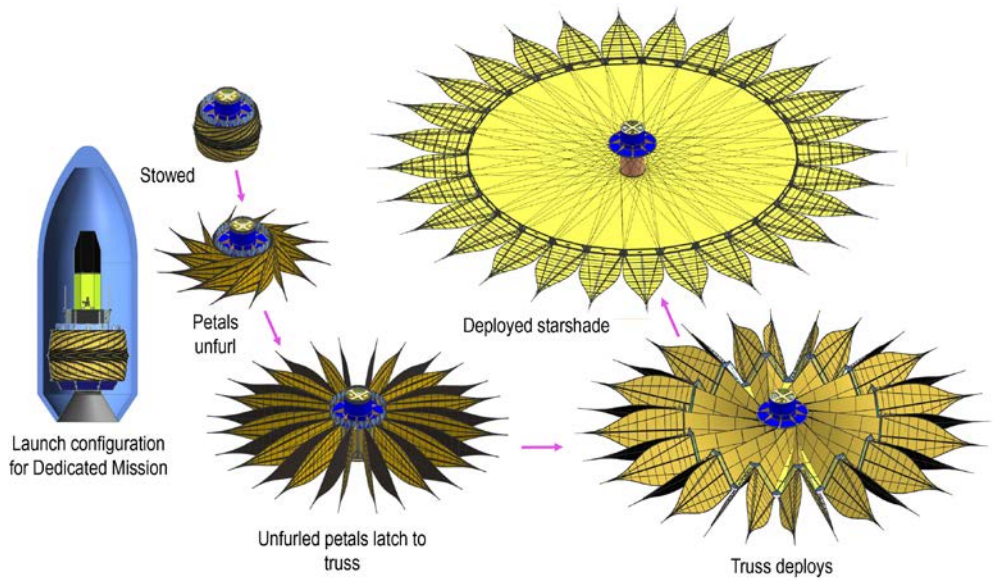

Figure 7. Starshade deployment sequence.

budget. Ratios above a certain threshold are avoided in the design for this same reason. This has the effect of loosely coupling the inner disk diameter to the number of petals (for a specified petal length); consequently, the number of petals and inner disk diameter must be determined jointly through both optical and mechanical analyses. Finally, with the perimeter truss architecture, petal length is limited by a storage and deployment constraint requiring that the petals not overlap themselves when in the stowed configuration.

4. STARSHADE MISSION OPTIONS

4.1 The Range of Starshade Mission Concepts

The starshade mission concept has a range of options: a range of starshade sizes have been discussed from a small starshade on order of 30 m in diameter that would work with a 1.1-m-diameter aperture telescope, through a 70-m starshade that would have gone with the JWST [26], all the way up to a >100-m-diameter starshade that would be considered for several mission options, with the design points used to characterize the starshade architecture tradespace for the Exo-S study captured in Table 3.

Mission					Telescope/Starshade			Instrumentation		
Orbit	**#**	**Case Name**	**Mission Class/ Duration**	**Cost ($M FY15)**	**Tele-scope**	**Retarget Prop. Responsibility/ Technology**	**Starshade**	**Implementation**	**FOV**	**Optical Thru-put**
Earth Leading	**1A**	**Dedicated Case Study**	**B 3 years**	**~1100**	1.1-m NextView	Telescope SEP	16-m disk 22 7-m petals	Dedicated IFS Dedicated Imager	30 arcsec 60 arcsec	42% 51%
	1B	Dedicated Downgrade	C 3 years	~950						
	1C	Dedicated Tech Demo	D 1 year	~750	0.6-m QuickBird	Telescope Small Biprop	16-m disk 22 6-m petals			
Earth-Sun L2	2A	Rendezvous Hi Performance	B 5 years	~800	2.4-m WFIRST/ AFTA	Starshade SEP*	20-m disk 22 9-m petals	Dedicated IFS Dedicated Imager	30 arcsec 60 arcsec	42% 51%
	2B	Rendezvous Upgrade	C 3 years	~640		Starshade Large Biprop	20-m disk 28 7-m petals			
	2C	**Rendezvous Case Study**	**C 3 years**	**~630**				Coronagraph IFS Coronagraph Imager	2 arcsec 10 arcsec	22% 28%
	2D	Rendezvous Tech Demo	D 1 year	~400		Starshade Small Biprop				

Table 3. Starshade mission options, including two case study missions (1A & 2C) detailed in the Exo-S STDT Final Report.

4.2 Starshade Dedicated Mission

The Dedicated Mission concept (Option 1A in Table 1) looks at the low cost, end-to-end starshade direct imaging mission prescribed by the Exo-S study charter. The variations (not described here) have differing degrees of reliability and risk, and corresponding differences in cost, mission duration, and science value. The Dedicated Mission case is a Class B mission with a 3-year baseline mission duration (the spacecraft carries fuel for 5 years). Figure 7 shows the launch configuration.

The Dedicated Mission has a heliocentric Earth-leading, Earth drift-away orbit; repositioning telescope spacecraft; and purpose-built imaging system. For low-disturbance orbits capable of supporting multiday spacecraft alignment on a fixed target, the choices are Earth drift-away or L2. Earth drift-away was the better choice because it has lower gravity disturbances. Limited mission life and low data volumes make the drift-away's inferior communications link a non-issue. Repositioning the telescope spacecraft is the lower propellant choice. And as "dedicated" missions serving only starshade direct imaging objectives, the instruments for all three options are designed specifically for starshade science.

The launch vehicle first deploys the telescope spacecraft in its operational orbit, then maneuvers to the nominal separation distance, spins up, deploys the starshade, and finally maneuvers away. The starshade spacecraft acquires a safe Sun-pointed attitude. The starshade deployment is ground commanded.

The reference telescope design is based on the 1.1-m NextView telescope developed for commercial Earth imaging. Several of these telescopes are operational and the telescope is considered a current product line. The as-built telescope is highly compatible with starshade requirements and only limited modification is necessary. The most significant modification is the addition of a sunshade to allow pointing near the Sun without sunlight entering the barrel.

The telescope spacecraft bus is based on the Kepler bus. The telescope spacecraft provides the propulsion to retarget and control formation. The existing hydrazine propulsion system is used for formation control, with a change to slightly larger propellant tanks and the addition of more thrusters. Retarget maneuvers use the XIPS-25 ion engine and xenon propellant. This electric propulsion system is needed due to the limited mass available for retargeting propellant stemming from the cost-driven shared launch configuration, and is an addition to the Kepler-based design.

The starshade spacecraft is a simplified version of the WISE bus. It is spin-stabilized so no reaction wheels are needed. Power is generated via fixed body-mounted solar panels. There is no science data handling. direct-to-Earth communications are limited to engineering functions only. A small hydrazine propulsion system provides pointing and spin- control. The bus structure is ESPA (EELV [evolved expendable launch vehicle] secondary payload adapter) ring-based and provides the separation interface to the starshade.

3.3 Starshade Rendezvous Mission

The Starshade Rendezvous Mission leverages a separately funded space telescope to provide excellent science at a low cost. The starshade launches separately to *rendezvous* with the telescope, after telescope primary objectives are met. Consequently, the telescope must be in an orbit that enables the later rendezvous of the starshade. The telescope spacecraft (Figure 8) must also carry some specific hardware needed for formation flying. A formation guidance channel (FGC)—optics and a detector capable of sensing a laser beacon on the starshade—is essential and can be either a modification of an existing science instrument or included in a stand-alone starshade instrument. In addition to the FGC, an interspacecraft radio link is needed for spacecraft-to-spacecraft communications and as a formation flying ranging sensor. A science camera and spectrometer can be either purpose-built for starshade direct imaging or, if similar capabilities exist in the telescope spacecraft's payload, the instruments may be modified if necessary and repurposed for starshade science. Compliance with these requirements constitutes a "starshade ready" telescope.

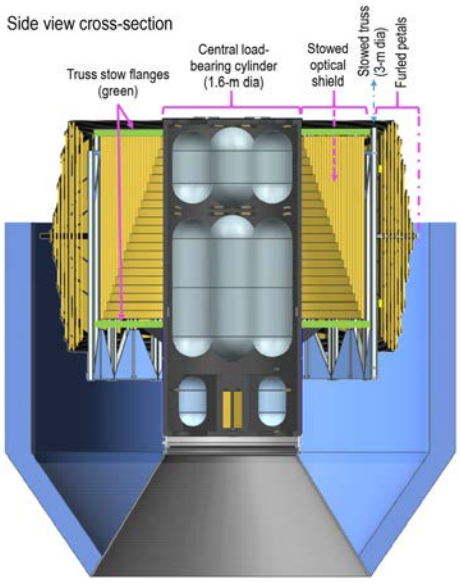

Figure 8. Rendezvous starshade spacecraft launch configuration.

WFIRST-AFTA has been adopted as the Rendezvous Mission's telescope reference design for the Exo-S study. The Rendezvous Mission design looks to minimize the impact on WFIRST-AFTA; no stringent requirements are imposed on the telescope spacecraft. The existing coronagraph instrument performs both science and formation guidance functions without adding focal planes. It is assumed, for the purpose of this study, that WFIRST-AFTA conducts its primary mission at Earth-Sun L2. The starshade is not launched unless the telescope is operational.

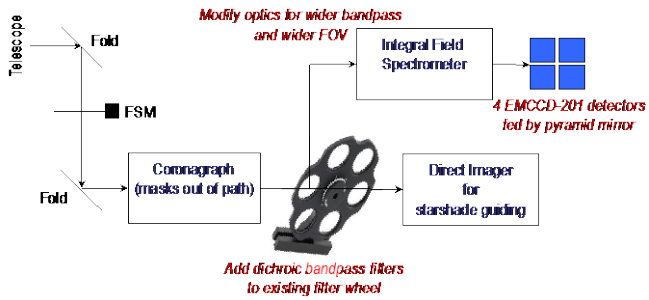

Figure 9. Block diagram of the WFIRST-AFTA coronagraph modified to perform starshade science and guidance functions. (Modifications described in red text.) Shown in IFS mode with Direct Imager used for formation guidance. Other filters use Direct Imager for science and IFS for formation guidance.

The Rendezvous Mission concept is designed as a Class C mission with a 3-year mission duration. It launches into an Earth-Sun L2 orbit. Telecommunications is handled by the Deep Space Network (DSN) as in the Dedicated Mission, but the Rendezvous Mission uses the telescope asset as a data relay with the DSN. The Rendezvous starshade

spacecraft does the repositioning from target to target, and not the telescope spacecraft as for the Dedicated Mission. The starshade uses the WISE-based spacecraft bus design as for the Dedicated Mission.

The telescope reference design is WFIRST-AFTA. The current Rendezvous Mission design allowable Sun off-point angles do not completely overlap with those of WFIRST-AFTA. Starshade observations are constrained to within 83° of Sun, to keep sunlight off any telescope facing starshade surface, and greater than 40° from Sun, to keep sunlight out of the telescope barrel. By comparison, the baseline WFIRST-AFTA Sun pointing constraint is 126° to 54°, based upon sizing of the fixed solar array for a geosynchronous orbit mission. It is assumed that a redesign for an Earth-Sun L2 mission affords the opportunity to increase the WFIRST-AFTA solar array and sunshade size consistent with the starshade goal. Looking to keep the mass, power, and testing impacts to a minimum, the Rendezvous Mission case study adopted a no-new-optical-channel rule when modifying the current WFIRST-AFTA design to support starshade science. Modest changes were needed in the coronagraph's IFS (Figure 9). See [27] for more details.

The starshade spacecraft performs the retarget and formation control maneuvers with a conventional bipropellant propulsion system. Propellant and pressurant tanks are installed inside the starshade central cylinder. The Rendezvous mission starshade spacecraft configuration is shown in Figure 8.

5. STARSHADE RENDEZVOUS EARTH FINDER MISSION

After completion of the Exo-S Probe study, an enhanced mission option that is design to focusing on exoEarth discovery was studied, called the "Starshade Rendezvous Earth Finder Mission". This is an enhanced option over the Rendezvous Mission case study detailed above (option 2C in Table 2) is a 3-year Class C mission that broadly targets all planet types and emphasizes low cost and technology readiness over science performance. The starshade is 34-m in diameter to match current prototypes and retarget maneuvers are performed with conventional chemical propulsion.

Here we introduce a 5-year Class B Rendezvous Mission (option 2A) that focuses on detecting Earth-like planets, but will detect planets of all types. Retarget maneuvers are performed with solar electric propulsion. The approach is to find the optimal balance between IWA and observing bandwidth, within constraints on propulsive acceleration, launch mass capacity and telescope observing time. Smaller observing bandwidths allow smaller IWAs that dramatically increase HZ access. The benefit is diminished by increased integration times, retarget times and propellant mass, due to reduced photon flux and increased starshade-telescope separation distance. A modest increase in starshade diameter to 40-m is also considered as a means to reduce IWA. The benefit is again diminished by increased retarget times and propellant consumption, due to increased separation distance and starshade mass.

The starshade performs retarget maneuvers with advanced Hall-Effect thrusters in development for the Asteroid Redirect Mission (ARM). This thruster is designed for much larger throughput capacity than is required here and delivers an efficient combination of thrust (526-mN) and specific impulse (3,000-s). It requires 13.3-kW of power at 800-V and

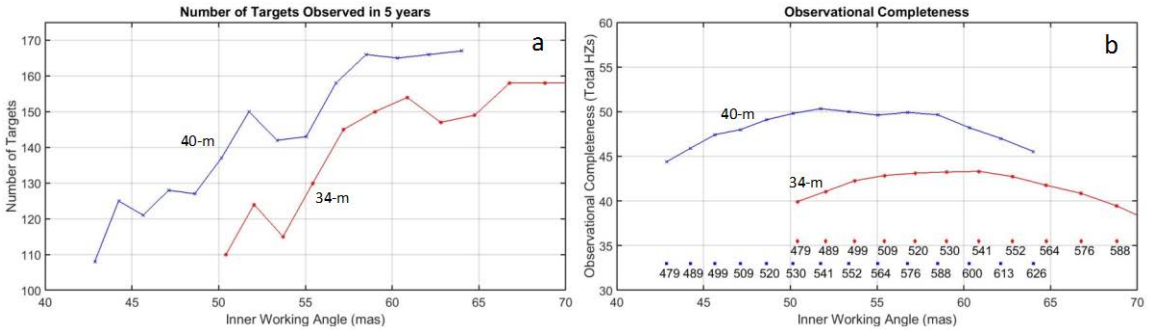

Figure 10. Number of targets observed and observational completeness for a 5 year mission utilizing 25% of the on-sky time of a 2.4 m telescope. a) Number of targets observed for 40-m and 34-m starshades assuming detection with the WFIRST-AFTA coronagraph camera. b) Curves show observational completeness. At any IWA, the optical bandpass ranges from 400 nm to the value indicated by the points labeled at the bottom of the graph. The lower set of values is for the 40-m and the higher set is for the 34-m.

consumes xenon gas. This power is provided by thin-film solar cells integrated into the optical shield of the starshade inner disc. A Falcon-9 launch vehicle delivers up to 3,700 kg to Earth-Sun L2 on a direct trajectory. Telescope observing time is limited to 25% of WFIRST mission time, during the period of starshade operation.

The instrument approach and optical throughput performance is another variable considered. One option is to use the existing AFTA coronagraph, with 28% optical throughput, after rotating the coronagraph masks out of the path. A second option is to use a dedicated instrument with an optical throughput of 46% [27].

For a given IWA, the starshade is capable of achieving the required contrast over a limited bandpass [28]. The lower wavelength limit is 400 nm, at the sensitivity limit of the AFTA coronagraph [29]. For each combination of IWA and bandpass, the DRM tool [21] is used to generate a ranked list of targets for detecting Earth-like planets based on habitable zone search completeness and integration time. Search completeness is computed for a planet sensitivity of 26 stellar magnitudes relative to the parent star. The total observational completeness is estimated as the sum of target search completeness consistent with observing 25% of the time over 5-years. Here we assume that the WFIRST-AFTA coronagraph optics are used and that the coronagraph masks are folded out of the beam. The instrument throughput is 28%.

Preliminary results for two starshade diameters (34-m and 40-m) are shown in Figure 10. The left plot shows the total number of targets and right plot shows the total observational completeness. Each curve reflects the combination of all constraints. The number of targets observed increases with IWA. At large IWA, the starshade is closer to the telescope and the bandwidth is wider so that integration times are shorter; both of these factors allow more targets to be observed. However, the average observational completeness of this larger sample of targets is reduced compared to observations of fewer targets at smaller IWAs. This leads to an optimum choice of IWA and bandwidth as shown in Figure 10b. A 40-m starshade observes ~50 HZs with IWA = 52 mas and bandpass 400-540 nm. The number of targets at maximum HZ completeness is in the range of 150-160 (30-32 yr^{-1}) depending on the configuration.

This study shows that a moderate size starshade with a 2.4 m telescope can perform compelling science with a significant yield of Earth-like planet detections. Assuming $\eta_{Earth} = 0.2$, the expected number of imaged exoEarths is about 10. An abundance of other planet types will also be detected. A subset of the detected planets can also be characterized over wider bandwidths, but with larger IWAs.

6. TECHNOLOGY DEMONSTRATIONS, CHALLENGES, AND DEVELOPMENT PLANS

Full-scale, ground-based end-to-end testing is not possible for the full starshade-telescope system; rather, it is replaced by a two-step process. First, metrology tests of the full-scale flight starshade will verify that the starshade will have the correct shape on-orbit. Second, subscale testing will demonstrate a dark shadow in broadband light in the lab and validate the optical model to the required levels of a few times 10^{-11} contrast. A third category of technology is formation flying at tens of thousands of km distance. The major technical challenges must be considered in light of flight-proven technologies for analogous commercial large deployable antenna systems. Table 4 outlines the key technology development status. For a description of the error budget see [30].

Key Challenges	Driving Specification	Technology Status
Dynamic stability	Deformations < 15 ppm after 10 s	Verified by analysis with large margins
Thermal stability	Non-uniform deformations ≤ 10 ppm	Verified by analysis with large margins
Manufacturing tolerance	Petal width < 100 μm (4 mil)	Demonstrated per TDEM-09
Deployment tolerance	In-plane petal root position ≤ 0.5 mm	Demonstrated per TDEM-10
Edge-scattered sunlight	Edge radius curvature <1 μm	Demo in progress per TDEM-12
Laboratory contrast demo and model validation	10^{-10} contrast at flight Fresnel Number	Demo in progress per TDEM-12
Formation flying	Sensing for lateral control ±1 m	Requires technology demonstration

Table 4. Technology challenges and status.

6.1 Starshade Manufacturing and Deployment

Key technology challenges, once considered tall-pole issues, but now considered demonstrated are: precision petal manufacturing, precision deployed positioning, and on-orbit stability.

Petals must be precisely manufactured to the specified petal width profile, or optical apodization function (with tolerance ≤ 100 μm). This capability was successfully demonstrated by a Technology Development for Exoplanet Missions (TDEM) activity (see Figure 11).

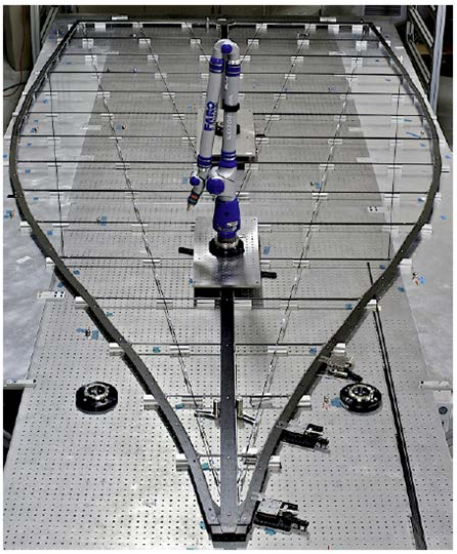

Figure 11. Petal prototype (TDEM-09) used to demonstrate manufacturing tolerance on petal width profile. The measured petal shape error (green arrows) vs. 100 μm met the allocated tolerance tolerance for 1×10^{-10} imaging.

Petals must be precisely deployed to the specified petal root positions, as controlled by the perimeter truss (in-plane root positions ≤ 500–750 μm). This capability was successfully demonstrated by a TDEM activity (see Figure 12 and Figure 13).

Petal width profiles must be precisely maintained on-orbit (non-uniform thermal deformations ≤10 ppm). This capability was successfully demonstrated by analysis. Predicted deformations are a small fraction of allocations. Dynamic deformations are also allocated and successfully demonstrated by analysis with large margins, aided by the structural attenuation and damping provided by the starshade. Dynamic deformations are allocated after some transient period during which larger deformations are acceptable because they are not sensed by the instrument.

Development of the starshade optical shield blanketing system is a technology area under study.

6.2 Starlight Contrast, Suppression, and Diffraction Verification

Starshade optical performance tests aim to demonstrate contrast (image plane) and suppression (pupil plane) performance consistent with imaging exoEarths and will validate the optical models via subscale experiments, upon which full-scale shape tolerance allocations are based. The scaling approach is to match the flight design in terms of the number of Fresnel zones to within a factor of ~2 and to also match the number of resolution elements across the starshade, so that the diffraction equations defining the dark shadow are representative of the mission.

Several experiments over the last decade have made progress toward demonstrating the viability of creating a dark shadow with a starshade, including: the University of Colorado [31, 32]; Northrop-Grumman [33]; Princeton University [34, 35]; and larger scale tests in a dry lake bed [36] Each of these experiments is limited in contrast and suppression performance to some extent by one or more of the following test environment issues: wavefront errors due to collimating optics; diffraction effects due to the finite extent of the optical enclosure; diffraction off starshade support struts; dust in open air testing, both airborne and contaminating the starshade edge; and size limitations resulting in large Fresnel number and overresolved images. To date, laboratory demonstrations in the testbed at Princeton at 0.1% scale have achieved monochromatic contrasts better than 10^{-10} levels (IWA=400 mas, Fr>600) [35]. Starshade field testing in the desert testing has demonstrated detection of source equivalent to a planet at roughly 10^{-8} contrast at km scale (IWA=70 as; Fr=240) with a 50% bandpass [36]. New field tests using the McMath solar observatory housing have reached better than 10^{-8} with similar IWA and Fr numbers (S. Warwick, priv. comm. 2015).

Future work is underway to address optical performance verification and model validation. A new TDEM activity (TDEM-12) led by N. J. Kasdin involves the development and testing of an improved subscale starshade with more precise edge shape and optical edge RoC ≤ 1 μm is the first priority. A completely new and much improved optical testbed at Princeton is planned with length greater than 70 m. The goal is to achieve a Fresnel number within a factor of 2 of the baseline flight design with IWA about 80 mas. The starlight simulator will also be capable of producing broadband light. A separate TDEM-12 activity led by T. Glassman of NGAS aims to improve upon the open air testing of larger starshades, on the order of 1 m in diameter. The test objectives include characterizing and modeling sensitivity to lateral control errors and the benefit of spinning the starshade. Other field testing of starshades on order of 10 cm at McMath Solar Observatory will reach flight-like Fr numbers (but still with large IWA) (S. Warwick, priv. comm. 2015). Another new TDEM-13 activity led by Professor W. Cash of the University of Colorado, Boulder features meter-class starshades for further testing on dry lake beds and in the 500 m XRCF vacuum beamline facility at the Marshall Space Flight Center.

Figure 12. Deployed position tolerance demonstration. Petal root positions are measured after each of 20

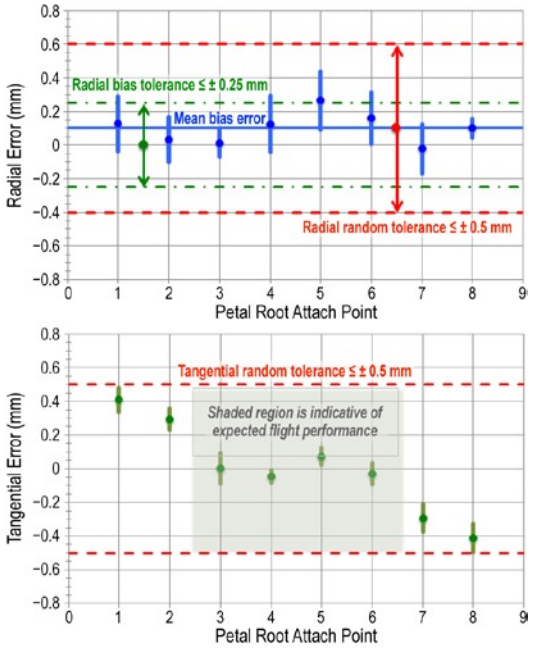

Figure 13. Measured deployment errors (3 σ with 90% confidence) are all within tolerance allocations.

Control of edge-scattered sunlight, and development of the starshade optical shield (OS) blanketing system and activities are funded to address these issues.

6.3 Formation Flying

The Exo-S formation flying at tens of thousands of km separation from the telescope is needed to keep the telescope positioned within the dark shadow created by the starshade. More specifically the starshade is designed to produce a dark shadow that extends radially only 1 m beyond the telescope aperture. Contrast degrades rapidly beyond the 1-m specification, so the starshade's position must be held to a lateral tolerance of ±1 m (Figure 14). The lateral tolerance requirement at tens of thousands of km is the driving requirement. Additionally, the starshade-telescope separation distance must be kept within ±250 km for effectiveness of the optical bandpass.

The Exo-S formation flying operational design utilizes three distinct modes all using the RF link to measure interspacecraft range. The Transition mode covers the activities needed to move the observatory between target stars and

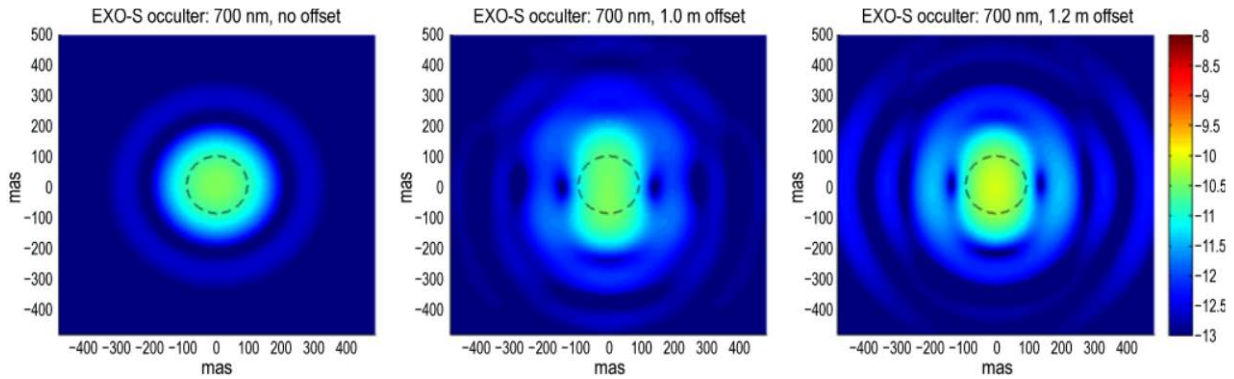

Figure 14. Image plane contrast in orders of magnitude at 700 nm with no lateral error (left), 1 m error (center), and 1.2 m error (right). The dashed circle indicates the inner working angle.

uses an LED (light-emitting diode) array on the starshade and a star tracker on the telescope for bearing measurements to autonomously navigate between target stars. Second, acquisition mode covers the establishment of co-alignment of the starshade spacecraft and the telescope spacecraft on the new target star. Science mode addresses the maintenance of the starshade and telescope alignment during science observations. Bearing measurements in Science mode use a laser beacon on the starshade that is observed by the formation guidance channel (FGC) within the imaging instrument of the telescope. (Note: the FGC function is carried out by the coronagraph imaging camera in the Rendezvous concept). The FGC and laser beacon are collectively referred to as the fine bearing sensor system (FBS). Starlight outside of the band of observation diffracts around the starshade and is collected by the telescope and detected by the FGC. By sensing both this out-of-band starlight and the starshade's laser beacon, the Science mode adjusts the lateral position of one of the spacecraft to align the two light sources, thus keeping the two spacecraft in formational alignment with the target star. Acquisition mode controls the handoff between the LED/star tracker system used to sense bearing in the Transition mode, and the FBS used to measure bearing in the Science mode. See Figure 15 for further description.

Formation flying at distances of tens of thousands of kilometers for lateral control at ±1m appears daunting and is an issue that has not been previously demonstrated. Controlling relative spacecraft positions to 1 m for Science mode is not a technological challenge; docking at the ISS requires control to better than 30 cm. The disturbing gravity gradients for a starshade mission are comparable to those experienced during ISS docking through the gravity gradient in low Earth orbit (LEO) at 1 m of separation just prior to docking. It is important to recognize that the disturbance environment is very benign in either a heliocentric Earth-leading, Earth drift-away orbit or an L2 orbit. Solar pressure is the dominant disturbance and permits a very low control bandwidth. This contributes to improving formation-sensing accuracy by allowing long sensor integration times.

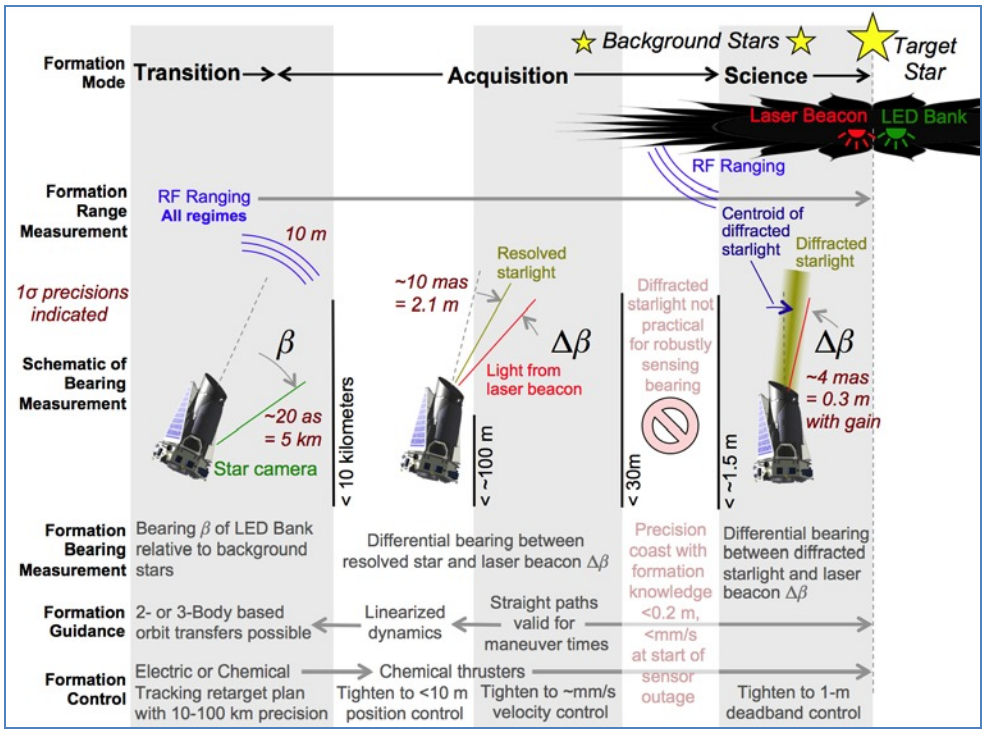

Figure 15. Formation flying modes and description.

Sensing is another matter: typically, positions must be sensed to 3 to 5 times more finely than the control requirement. Sensing to a factor of three finer than control implies that the lateral offset of the starshade must be sensed to 30 cm at 50 Mm. This offset corresponds to a bearing measurement precision of 6 nrad (1.25 mas).

The 6 nrad precision bearing sensing capability is the major challenge for formation flying. Three factors help with the bearing sensing requirement. One, the large telescope aperture collects a large number of photons (10k to 100k per second) both from the beacon and from the stellar leakage; bearing knowledge improves with the square root of the

number of photons. Two, the large aperture has an intrinsically high angular resolving power. Three the apparent starshade offset is magnified by a geometrical effect.

A demonstration of the precision-bearing sensing capability is under way (TDEM-13 led by Prof. J. Kasdin). A breadboard formation sensing and control instrument, including FGC and image processing algorithms, will be built and then integrated into the Princeton starshade optical testbed. The detector will be mounted on a 2-axis stage to simulate lateral position errors. Simulations will be used to estimate performance and explore optimal formation control and acquisition strategies with the goal of a validation of formation flying to flight-like levels using real hardware in the loop.

6.4 Technology for the Starshade Rendezvous Earth Finder Mission

The Starshade Rendezvous Earth Finder Mission introduced in Section 5 has a few technology differences as compared with the mission options described in the Exo-S Final Report. The 40-m starshade consists of 8-m petals and a 24-m inner disk versus the current Rendezvous 34-m design with 7-m petals and a 20-m inner disk. This 14% increase to petal length and 20% increase to disc diameter is considered well within the scalable range of the current TRL-5 prototypes. The ARM thruster and power supply is currently in testing for TRL-5 and is targeted for a 2021 launch date. The incorporation of thin-film solar cells into the inner disc optical shield is included in the proposed TDEM-14 activity. The cells are expected to add less than 10% to the optical shield mass and are not expected to interfere with deployment dynamics. One issue will be demonstrating radiation tolerance of the thin-film cells. A significant advantage is that the inner disk area is more than twice the area required for even the thinnest and lowest efficiency cells under consideration, such that a large amount of radiation degradation can be accommodated.

7. SUMMARY

The starshade-telescope system probe-class mission offers a breakthrough opportunity for space-based exoplanet direct imaging: compelling science can be returned at the same time as the technological and scientific framework is developed for a larger flagship mission. The starshade can reach to the discovery of Earth-size planets in the habitable zones of nearby stars using a relatively small space telescope. This capability is due to the planet-star flux contrast and IWA being nearly independent from the telescope aperture size. The starshade is responsible for blocking the starlight, enabling a non-specialized space telescope.

8. ACKNOWLEDGEMENTS

The contents of this manuscript are largely drawn from the Exo-S report http://exep.jpl.nasa.gov/stdt/Exo-S_Starshade_Probe_Class_Final_Report_150312_URS250118.pdf, funded through the NASA's Exoplanet Exploration Program. The work reported here was performed in part at the Jet Propulsion Laboratory, California Institute of Technology, under a contract with the National Aeronautics and Space Administration.

9. REFERENCES

[1] Traub, W. A., "The colors of extrasolar planets," Scientific Frontiers in Research on Extrasolar Planets 294, 595-602 (2003).

[2] Karkoschka, E., "Spectrophotometry of the Jovian Planets and Titan at 300- to 1000-nm Wavelength: The Methane Spectrum," Icarus, 111(1), 174-192 (1994).

[3] Cahoy, K. L., Marley, M. S. and Fortney, J. J., "Exoplanet albedo spectra and colors as a function of plaent phase, separation, and metallicity," Astrophysical Journal, 724(1), 189-214 (2010).

[4] Robinson, T. D., Meadows, V. S., Crisp, D. *et al.*, "Earth as an Extrasolar Planet: Earth Model Validation Using EPOXI Earth Observations," Astrobiology, 11(5), 393-408 (2011).

[5] Vogelsberger, M., Genel, S., Springel, V. *et al.*, "Properties of galaxies reproduced by a hydrodynamic simulation," Nature, 509(7499), 177-182 (2014).

[6] Borucki, W. J., Koch, D., Basri, G. *et al.*, "Kepler planet-detection mission: Introduction and first results," Science, 327(5968), 977-980 (2010).

[7] Ricker, G. R., Winn, J. N., Vanderspek, R. *et al.*, "Transiting Exoplanet Survey Satellite (TESS)," Proc. SPIE 9143, 914320 (2014).

[8] Torrey, P., Snyder, G. F., Vogelsberger, M. *et al.*, "Synthetic galaxy images and spectra from the Illustris simulation," Monthly Notices of the Royal Astronomical Society, 447(3), 2753-2771 (2015).

[9] Spitzer, L., "The beginnings and future of space astronomy," American Scientist, 50(3), 473-484 (1962).
[10] Marchal, C., "Concept of a space telescope able to see the planets and even the satellites around the nearest stars," Acta Astronautica, 12(3), 195-201 (1985).
[11] Copi, C. J. and Starkman, G. D., "The Big Occulting Steerable Satellite (BOSS)," The Astrophysical Journal, 532(1), 581 (2000).
[12] Schultz, A. B., Jordan, I. J. E., Kochte, M. *et al.*, "UMBRAS: A matched occulter and telescope for imaging extrasolar planets," Proc. SPIE 4860, 54-61 (2003).
[13] Simmons, W. L., [A pinspeck camera for exo-planet spectroscopy] Princeton University, (2005).
[14] Simmons, W. L., Cash, W. C., Seager, S. *et al.*, [The New Worlds Observer: a mission for high-resolution spectroscopy of extra-solar terrestrial planets], (2004).
[15] Vanderbei, R. J., Spergel, D. N. and Kasdin, N. J., "Circularly symmetric apodization via star-shaped masks," Astrophysical Journal, 599(1), 686-694 (2003).
[16] Cash, W., "Detection of Earth-like planets around nearby stars using a petal-shaped occulter," Nature, 442(7098), 51-53 (2006).
[17] Vanderbei, R. J., Cady, E. and Kasdin, N. J., "Optimal occulter design for finding extrasolar planets," Astrophysical Journal, 665(1), 794-798 (2007).
[18] Cash, W., Kendrick, S., Noecker, C. *et al.*, "The New Worlds Observer: the astrophysics strategic mission concept study," 7436, 743606-743606-14.
[19] Kasdin, N. J., Cady, E. J., Dumont, P. J. *et al.*, "Occulter design for THEIA," 7440, 744005-744005-8.
[20] Hillenbrand, L. A., Carpenter, J. M., Kim, J. S. *et al.*, "The complete census of 70 mu m-bright debris disks within "the formation and evolution of planetary systems" Spitzer legacy survey of sun-like stars," Astrophysical Journal, 677(1), 630-656 (2008).
[21] Trabert, R., Shaklan, S. B., Lisman, P. D. *et al.*, "Design reference missions for the Exoplanet Starshade (Exo-S) Probe-Class study," Proc. SPIE 9605(2015).
[22] Lindler, D. J., "TPF-O design reference mission," Proc. SPIE 6687, 68714 (2007).
[23] Hunyadi, S. L., Lo, A. S. and Shaklan, S. B., "The dark side of TPF - detecting and characterizing extra-solar Earth-like planets with one or two external occulters - art. no. 669303," Proc. SPIE 6693, 69303 (2007).
[24] Savransky, D., Kasdin, N. J. and Cady, E., "Analyzing the Designs of Planet-Finding Missions," Publications of the Astronomical Society of the Pacific, 122(890), 401-419 (2010).
[25] Glassman, T., Newhart, L., Voshell, W. *et al.*, "Creating optimal observing schedules for a starshade planet-finding mission," Aerospace Conference, IEEE, 1-19 (2011).
[26] Soummer, R., Valenti, J., Brown, R. A. *et al.*, "Direct imaging and spectroscopy of habitable planets using JWST and a starshade," Space Telescopes and Instrumentation 2010: Optical, Infrared, and Millimeter Wave, 7731, 15 (2010).
[27] Martin, S. R., Cady, E., Shaklan, S. B. *et al.*, "Optical instrumentation for science and formation flying with a starshade observatory," Proc. SPIE 9605(2015).
[28] Cady, E., "Nondimensional representations for occulter design and performance evaluation," Proceedings of SPIE, 8151, 815112-815112-10 (2011).
[29] Tang, H., "The WFIRST/AFTA Coronagraph instrument optical design," Proc. SPIE 9605(2015).
[30] Shaklan, S. B., Marchen, L., Cady, E. *et al.*, "Error budgets for the Exoplanet Starshade (Exo-S) probe-class mission study," Proc. SPIE 9605(2015).
[31] Schindhelm, E., Shipley, A., Oakley, P. *et al.*, "Laboratory studies of petal-shaped occulters," Proc. SPIE 6693, 69305 (2007).
[32] Leviton, D. B., Cash, W. C., Gleason, B. *et al.*, "White light demonstration of one hundred parts per billion irradiance suppression in air by new starshade occulters," Proc. SPIE 6687, B6871 (2007).
[33] Samuele, R., Glassman, T., Johnson, A. M. J. *et al.*, "Starlight suppression from the starshade testbed at NGAS," Proc. SPIE 7440, 744004 (2009).
[34] Cady, E., Balasubramanian, K., Carr, M. *et al.*, "Progress on the occulter experiment at Princeton," Proc. SPIE 7440, 744006 (2009).
[35] Sirbu, D., Kasdin, N. J. and Vanderbei, R. J., "Monochromatic verification of high-contrast imaging with an occulter," Optics Express, 21(26), 32234-32253 (2013).
[36] Glassman, T., Casement, S., Warwick, S. *et al.*, "Measurements of high-contrast starshade performance," Proc. SPIE 9143, 91432 (2014).